An Integrated Finite Element Procedure for ComputerModelling of Tension Structures

B. Tabarrok and Z. Qin[1]

This paper presents an integrated finite element procedure for computer-aided design and analysis of tension structures. Three distinct phases in the design of tension structures, namely, form finding, stress analysis and cutting pattern generation, are addressed and numerical approaches to each phase are outlined. Some numerical examples are given to illustrate the applications of the newly developed finite element program package, NATS (Nonlinear Analysis of Tension Structures).

INTRODUCTION

Considerable advances have been made in the computer modelling of tension structures in recent decades. Various computational methods have been developed to assist engineers in the design of tension structures [1-10] and solutions of some problems are still under development [11-16].

In general, the computer-aided design and analysis of tension structures fall into three distinct phases, form finding, stress analysis and cutting pattern generation. The form finding phase seeks to establish the equilibrium configuration for the structure that conforms to the functional and structural requirements. On completion of form finding, the performance of the structure under a number of design load cases is analyzed. This enables the determination of fabric, frame and cable design stresses and deflections. Once a satisfactory shape has been found, cutting patterns which determine the shapes of fabric strips, in a plane, to form the 3-D surface of the structure, may be generated.

The above three phases involved in the design of tension structures can be carried out by applying the finite element method. To this end, we have developed a large-displacement finite element analysis program for both form finding and stress analysis phases. Since tension structures incorporate a combination of membranes, cables and frames, three types of elements, namely, membrane, cable and beam, are developed. The membrane elements are so formulated as to remove compressive stresses – a condition that gives rise to membrane wrinkling. To account for orthotropic properties of the fabric membrane, varying properties are assigned to the warp and weft directions. Various types of loading are considered in the stress analysis.

The cutting pattern generation is based on a weighted least-squares minimization flattening approach. A computer method is developed for simultaneous form finding and cutting pattern generation which produces initial principal stresses in the directions of the warp and weft of the fabric. This is accomplished by first dividing the membrane surface into individual

1. Department of Mechanical Engineering, University of Victoria, Victoria, B.C., Canada.

Scientia Iranica, Vol. 2, No. 1, © Sharif University of Technology, March 1995.

cloth layouts and then flattening it into plane strips. For best results, the cutting lines for the patterns are selected along the geodesics of the doubly-curved surface of the membrane.

MESH GENERATION

Before a finite element analysis of a structure can be performed, it is necessary to describe the geometry of the structure. For form finding of tension structures, a mesh is initially generated for the membrane on a flat plane. Then the membrane nodes to be attached to the frame, centerpole, etc., are displaced towards their final locations in 3-D space. For this purpose, a large displacement finite element analysis is carried out and the computed displacements are added to the initial coordinates. This approach, which uses meshing on a flat plane, dispenses with the need for the more difficult task of meshing a doubly-curved surface.

Mesh generation is started by first dividing the flat membrane into large triangular or quadrilateral subdomains with straight or curved boundaries. The boundaries of these subdomains may represent locations of cables and parts of the frame. The subdomains are then automatically meshed by a number of three-node triangular elements, based on the isoparametric mapping process [17]. Triangular elements defined within each region are used to represent the membrane, while line elements represent cable and beam elements along the boundaries.

Most fabric materials used in tension structures have orthotropic properties and normally the initial stresses are applied along the warp and the weft directions. Since no shear stresses are imposed, the initial stresses are principal stresses and the warp and weft directions, in the flat state, are principal directions. For purposes of generating cutting patterns, it is again useful to use the principal directions. To this end it is expedient to lay out the elements in a pattern such that the element x axis lies along one of the principal directions, which we take as the warp direction. The element y axis is taken perpendicular to that

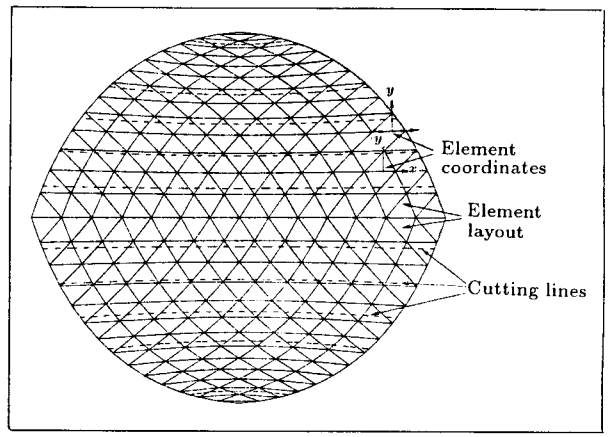

Figure 1. Initial mesh.

direction. Thus, the local element coordinate system is coincident with the material principal directions, as shown in Figure 1. In such a local coordinate system, different material constants can be specified and nonuniform initial stresses may be prescribed.

FORM FINDING

For normal structures, the configuration is known a priori. This is not the case for tension structures. Tension structures are usually constructed with a significant prestress at all times. Thus, there is generally no unstressed configuration for the entire structure, even if no external loads are applied and the self-weight of the structure is neglected. Since the membrane in a tension structure possesses no flexural stiffness, its form or configuration depends upon the tension in the membrane. Thus, the load bearing behavior and the shape of the membrane cannot be separated and cannot be described by simple geometric models. The membrane shape, the load on the structure and the internal stresses interact in a nonlinear manner to satisfy the equilibrium equations.

The preliminary design of tension structures involves the determination of an initial configuration in which the specified prestresses are in equilibrium. In addition to satisfying the equilibrium conditions, the initial configuration must accommodate both architectural (aesthetics) and structural (strength and sta-

bility) requirements. Further, the requirements of space and clearances should be met, the membrane stresses must all be tensile to avoid wrinkling and the radii of the doubly-curved surfaces should be small enough to resist out-of-plane loads and to insure structural stability.

The finite element method provides the most versatile approach for analysis of tension structures. Owing to the geometric nonlinearity of membrane structures, it is preferable to use a dense mesh of flat primitive elements rather than a coarse mesh made up of flat higher order elements. To this end, the present work uses constant stress triangular membrane element with three nodes and three degrees of freedom per node. The cable and beam elements have two end nodes with six degrees of freedom for cable and 12 degrees of freedom for beam elements, respectively.

The procedure for form finding, using the large-displacement finite element analysis, is based on the same procedure as that used for analyzing the behavior of tension structures under various loads. The finite element equations of equilibrium are derived via the principle of virtual work, as follows:

$$\int_{A^e} \delta\epsilon^T \sigma h dA - \delta \mathbf{u}^T \mathbf{R} = \mathbf{0} \ , \tag{1}$$

where A^e is the element area, h is the thickness of the membrane, $\mathbf{u}$ is the displacement, ϵ is the strain, σ is the stress and $\mathbf{R}$ is the external nodal force.

The membrane is incapable of sustaining flexural stresses. Therefore, only stresses tangent to curved surfaces of the membrane act to equilibrate loads normal to the surfaces. As the loads change, the stresses and the local curvatures change to maintain equilibrium and these changes are accompanied by significant displacements and rotations of the surface. Thus, the small-deflection theory of linear elasticity is inapplicable and the quadratic terms in displacement-strain relations must be taken into account. The nonlinear displacement-strain relations can be expressed as:

$$\begin{aligned}
\epsilon_x &= \frac{\partial u}{\partial x} + \frac{1}{2}\left[\left(\frac{\partial u}{\partial x}\right)^2 + \left(\frac{\partial v}{\partial x}\right)^2 + \left(\frac{\partial w}{\partial x}\right)^2\right] \ , \\
\epsilon_y &= \frac{\partial v}{\partial y} + \frac{1}{2}\left[\left(\frac{\partial u}{\partial y}\right)^2 + \left(\frac{\partial v}{\partial y}\right)^2 + \left(\frac{\partial w}{\partial y}\right)^2\right] \ , \\
r_{xy} &= \frac{\partial u}{\partial y} + \frac{\partial v}{\partial x} + \left[\frac{\partial u}{\partial x}\frac{\partial u}{\partial y} + \frac{\partial v}{\partial x}\frac{\partial v}{\partial y} + \frac{\partial w}{\partial x}\frac{\partial w}{\partial y}\right] \ .
\end{aligned} \tag{2}$$

Because we are considering large displacements and small strains, the constitutive relations for linear elastic plane stress analysis may be used. Thus, we write:

$$\sigma = \mathbf{D}\epsilon + \sigma_0 \ , \tag{3}$$

where σ_0 denotes the initial stress vector and $\mathbf{D}$ is the matrix of elastic constants.

The finite element equilibrium equations are derived, following the conventional procedure [13]. The large-displacement finite element method provides a flexible means for form finding of tension structures. Several variations on this basic method have been suggested.

Form finding is performed by first establishing a mesh in a plane. The designer then specifies a simple prestress distribution. A three-dimensional form is created by displacing the support points until they attain their prescribed positions. Newton-Raphson iterations are used to obtain equilibrium configurations in the deformed structure. The resulting strains may give rise to unfavorable stresses if actual values of material constants are used. This problem is overcome through an adjustment step which involves the direct specification of a desirable prestress for the deformed structure [1]. In practice, the application of this method is limited because of the difficulty of specifying desirable prestresses. An improvement can be made by removing the incremental stresses due to deformations after each incremental iteration. The stresses in the last iteration step will be in equilibrium and may then be used as prestresses for the final equilibrium configuration. The resulting stresses can be changed by adjusting the incremental iteration steps [13].

Minimum surfaces are often used in the design of tension structures [6,11]. To create a minimum surface, a fictitious constitutive law which maintains a constant prestress, independent of any changes in strain, is used. Such a constitutive law corresponds to a zero Young's modulus (in practical applications, a very small Young's modulus is used to avoid numerical instability). If a uniform prestress is specified, then the configuration obtained will have the specified uniform prestress in equilibrium. It is well known that a uniform stress surface is a minimum surface. The advantage of the minimum surface is its aesthetically pleasing shape and the associated uniform tensile stress everywhere in the membrane. However, some design requirements, such as clearances, may preclude the use of minimum surface configurations. Since the mean curvature for a minimum surface is zero, such surfaces tend to be rather flat. Noting that the load bearing capacity of a membrane, normal to its surface, depends on its curvatures one can see that minimum surfaces will not always be desirable for tension structures.

The performance of minimum surfaces can be improved by applying cables on the surfaces. For cable reinforced membrane structures, the equilibrium configuration depends upon the cable layout and the ratio of the prestresses in the membrane to those in the cables. It has been shown that the principle of virtual work for cable-reinforced membrane structures, in the absence of external forces, is equivalent to the variational statement for minimum surface subject to an isorperimetric constraint requiring the constancy of the length between two points on the surface [13], namely:

$$\int_A \delta\epsilon^T \sigma h dA + \int_S \delta\epsilon_c \sigma_c A_c ds = \delta \int_A \Delta A dA + \lambda \delta \int_S \Delta l ds \ , \qquad (4)$$

where ϵ_c and σ_c are the strain and the stress in the cable, A_c is the cross-section area of the cable, ΔA and Δl are the membrane elemental area and the cable elemental length, and λ can be viewed as a penalty parameter, with a preassigned value, for the imposition of the constraint,

$$\lambda = \frac{\sigma_c A_c}{\sigma h} \ . \qquad (5)$$

It is evident from Equation 5 that λ is the ratio of the stresses in the membrane to that in the cable.

In some cases, a desirable non-uniform prestress distribution may be specified and, using a very small Young's modulus, one can create an initial equilibrium configuration with the specified non-uniform prestresses in equilibrium. Such non-uniform stress surfaces which are not minimum surfaces provide more flexibility for the designer [14]. However, it is not always obvious how one should preassign non-uniform prestresses for some tension structures.

To provide the designer greater choice in form finding of tension structures, a more flexible method has been developed. This method involves the application of an appropriate external pressure. The initial equilibrium configuration is obtained by displacing the support points and applying the specified external pressure simultaneously. The resulting equilibrating shape depends on the ratio of the initial stress to the external pressure. Once a desirable shape has been found, several more iterations are needed to eliminate the external pressure in small load steps and to find an equilibrating stress distribution associated with the resulting shape.

For this final stage, the actual values of Young's modulus for the membrane and cables are used. To obtain an appropriate stress distribution, the incremental stresses due to deformations, obtained after the removal of the external pressure at each iteration, are removed. The stresses in the last iteration will be in equilibrium. Because the pressure used for form finding is usually very small, the final self-equilibrium shape, after elimination of the pressure, will be only slightly different from the preliminary one, and the resulting non-uniform stresses will be of the same order as that of the initially specified uniform stress.

The method of form finding under an

external pressure is flexible and allows for an infinite variety of feasible shapes. The procedure is equivalent to obtaining a minimum surface subject to constraints of cable lengths on the surface and total volume covered by the surface [14]. The equivalence between the principle of virtual work for cable-reinforced membrane under an external pressure and the variational statement for minimum surface subject to the constraints may be expressed as:

$$\int_A \delta\epsilon^T \sigma h dA + \int_S \delta\epsilon_c \sigma_c A_c ds - \int_A \delta w p dA = \delta \int_A \Delta A dA + \lambda\delta \int_S \Delta l ds + \phi\delta \int_A w dA \ , \tag{6}$$

where w is the displacement of the membrane, p is the external pressure and ϕ is a penalty parameter imposing the constraint of total volume covered by the surface,

$$\phi = -\frac{p}{\sigma h} \ . \tag{7}$$

The form finding procedures are applied in design of different tension structures. Figures 2 and 3 show two examples of tension structures created by the form finding program.

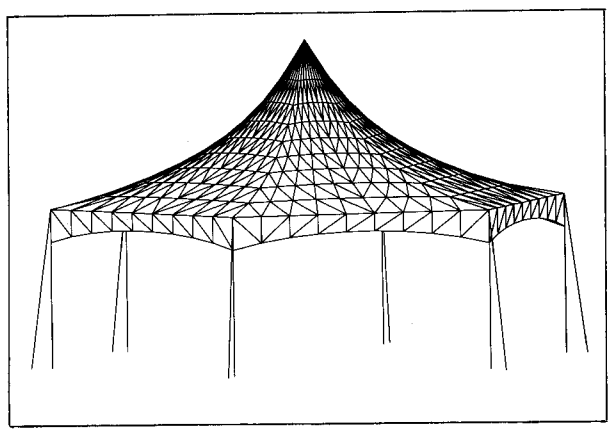

Figure 2. Initial configuration of hexagon tent.

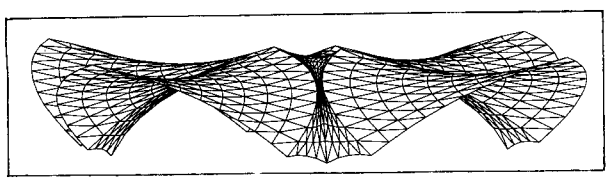

Figure 3. Initial configuration of clover-leaf tent.

STRESS ANALYSIS

Once the initial equilibrium shape is determined, the behavior of the structure under a variety of loads must be investigated to insure that the structure can withstand all the forces that it will encounter in service. The lack of flexural stiffness renders tension structures susceptible to large deflections, even under moderate loads. That is, such structures tend to adapt by undergoing large deflections under specified loads. In some cases, the loads themselves will be deformation dependent. An obvious example is pressure loading, which remains normal to the deflecting surface. A nonlinear analysis is required to include these effects in the load analysis of tension structures. Moreover, the membrane cannot resist any compressive stresses. Wrinkling will occur when the external loads give rise to compressive stresses larger than the initial tensile stresses. A procedure to treat element wrinkling should also be included in the load analysis.

The stress analysis program is basically the same as that for form finding. The finite element formulation is derived via the principle of virtual work, Equation 1. For a triangular membrane element, the displacements, in an element coordinate system (x, y, z), can be expressed as:

$$\begin{aligned} u(x,y) &= (a_1 + b_1 x + c_1 y)u_1 \\ &\quad + (a_2 + b_2 x + c_2 y)u_2 + (a_3 + b_3 x + c_3 y)u_3 \ , \\ v(x,y) &= (a_1 + b_1 x + c_1 y)v_1 \\ &\quad + (a_2 + b_2 x + c_2 y)v_2 + (a_3 + b_3 x + c_3 y)v_3 \ , \\ w(x,y) &= (a_1 + b_1 x + c_1 y)w_1 \\ &\quad + (a_2 + b_2 x + c_2 y)w_2 + (a_3 + b_3 x + c_3 y)w_3 \ , \end{aligned} \tag{8}$$

where:

$$a_1 = (x_2 y_3 - x_3 y_2)/2\Delta \quad b_1 = (y_2 - y_3)/2\Delta$$
$$c_1 = (x_2 - x_3)/2\Delta \ ,$$

$$a_2 = (x_3 y_1 - x_1 y_3)/2\Delta \quad b_2 = (y_3 - y_1)/2\Delta$$
$$c_2 = (x_3 - x_1)/2\Delta \ ,$$

$$a_3 = (x_1 y_2 - x_2 y_1)/2\Delta \quad b_3 = (y_1 - y_2)/2\Delta$$
$$c_3 = (x_1 - x_2)/2\Delta \ ,$$

and Δ denotes the area of a triangular element. Substituting Equation 8 into the displacement-strain relations, Equation 2, and writing them in matrix form, we have:

$$\epsilon = \mathbf{B}_0\mathbf{u} + \frac{1}{2}\mathbf{A}\boldsymbol{\theta} \ , \tag{9}$$

where:

$$\mathbf{B}_0 = \begin{bmatrix} b_1 & 0 & 0 & b_2 & 0 & 0 & b_3 & 0 & 0 \\ 0 & c_1 & 0 & 0 & c_2 & 0 & 0 & c_3 & 0 \\ c_1 & b_1 & 0 & c_2 & b_2 & 0 & c_3 & b_3 & 0 \end{bmatrix} \ ,$$

$$\mathbf{u} = [u_1 \ v_1 \ w_1 \ u_2 \ v_2 \ w_2 \ u_3 \ v_3 \ w_3]^T \ ,$$

$$\mathbf{A} = \begin{bmatrix} \partial u/\partial x & \partial v/\partial x & \partial w/\partial x \\ 0 & 0 & 0 \\ \partial u/\partial y & \partial v/\partial y & \partial w/\partial y \\ 0 & 0 & 0 \\ \partial u/\partial y & \partial v/\partial y & \partial w/\partial y \\ \partial u/\partial x & \partial v/\partial x & \partial w/\partial x \end{bmatrix} \ ,$$

$$\boldsymbol{\theta} = [\partial u/\partial x \ \ \partial v/\partial x \ \ \partial w/\partial x \ \ \partial u/\partial y \ \ \partial v/\partial y \ \ \partial w/\partial y]^T \ .$$

Thus:

$$\delta\epsilon = (\mathbf{B}_0 + \mathbf{AG})\delta\mathbf{u} \ , \tag{10}$$

where:

$$\mathbf{G} = \begin{bmatrix} b_1 & 0 & 0 & b_2 & 0 & 0 & b_3 & 0 & 0 \\ 0 & b_1 & 0 & 0 & b_2 & 0 & 0 & b_3 & 0 \\ 0 & 0 & b_1 & 0 & 0 & b_2 & 0 & 0 & b_3 \\ c_1 & 0 & 0 & c_2 & 0 & 0 & c_3 & 0 & 0 \\ 0 & c_1 & 0 & 0 & c_2 & 0 & 0 & c_3 & 0 \\ 0 & 0 & c_1 & 0 & 0 & c_2 & 0 & 0 & c_3 \end{bmatrix} \ .$$

Substituting Equations 3, 9 and 10 into Equation 1 and noting that $\delta\mathbf{u}^T$ is arbitrary, the vanishing of the virtual work expression reduces to:

$$\int_{V^e} (\mathbf{B}_0 + \mathbf{AG})^T [\mathbf{D}(\mathbf{B}_0\mathbf{u} + \frac{1}{2}\mathbf{A}\boldsymbol{\theta}) + \boldsymbol{\sigma}_0]dV - \mathbf{R} = \mathbf{0} \ . \tag{11}$$

The above equation provides the elemental equilibrium equations. These equations must be transformed to the global coordinates and finally assembled to obtain the global equilibrium equations. Since the global equations will be solved interatively by the Newton-Raphson method, we proceed to linearize the governing equations at the element level. To this end, we let:

$$\phi^i = \int_{V^e} (\mathbf{B}_0 + \mathbf{A}^i\mathbf{G})^T [\mathbf{D}(\mathbf{B}_0\mathbf{u}^i + \frac{1}{2}\mathbf{A}^i\boldsymbol{\theta}^i + \boldsymbol{\sigma}_0]dV - \mathbf{R} \ , \tag{12}$$

as the residual term after the ith iteration. Then, the tangent stiffness matrix of the membrane element may be written as:

$$\mathbf{K}^i_m = \frac{\partial\phi^i}{\partial\mathbf{u}} = \mathbf{K}^i_e + \mathbf{K}^i_g \ , \tag{13}$$

where $\mathbf{K}^i_e$ and $\mathbf{K}^i_g$ are the elastic stiffness matrix and the geometric stiffness matrix, respectively.

$$\mathbf{K}^i_e = \int_{V^e} (\mathbf{B}_0 + \mathbf{A}^i\mathbf{G})^T\mathbf{D}(\mathbf{B}_0 + \mathbf{A}^i\mathbf{G})dV \ , \tag{14}$$

and

$$\mathbf{K}^i_g = \int_{V^e} \mathbf{G}^T \frac{\partial(\mathbf{A}^i)^T}{\partial\mathbf{u}}\boldsymbol{\sigma}^i dV = \int_{V^e} \mathbf{G}^T\boldsymbol{\Sigma}^i\mathbf{G}dV \ , \tag{15}$$

where:

$$\boldsymbol{\Sigma}^i = \begin{bmatrix} \sigma_x & 0 & 0 & \tau_{xy} & 0 & 0 \\ 0 & \sigma_x & 0 & 0 & \tau_{xy} & 0 \\ 0 & 0 & \sigma_x & 0 & 0 & \tau_{xy} \\ \tau_{xy} & 0 & 0 & \sigma_y & 0 & 0 \\ 0 & \tau_{xy} & 0 & 0 & \sigma_y & 0 \\ 0 & 0 & \tau_{xy} & 0 & 0 & \sigma_y \end{bmatrix} \ .$$

The transformation of the element matrix, Equation 13, to global coordinates and the assembly of global stiffness matrix follow the conventional procedure. Now we move our attention to the external forces. In the present work, we define a load case as a combination of five different types of loading: (1) concentrated nodal loads, (2) dead loads (self-weight), (3) uniform pressure, (4) snow loads and (5) wind

loads. The specification of types (1) to (4) is straightforward, the computation of wind loads, however, is a complex problem. The wind loading requirements for tension structures are not currently adequately defined in building codes.

The design wind load for the structure is determined by using the following formula [18]:

$$p = q_z \times C_p \ , \tag{16}$$

where p is surface pressure on any part of the surface, q_z is velocity pressure and C_p is the pressure coefficient which depends on the wind direction and the current geometry of the surface. The velocity pressure q_z at height z is calculated from the formula:

$$q_z = 0.00256 \ K_z(I \times v)^2 \ , \tag{17}$$

where K_z is the exposure coefficient including gusts obtained from the Building Code, I is an importance factor and v is the wind speed measured as a fastest mile value.

The wind pressure coefficient C_p should be measured in wind tunnel experiments for each structural model, hence its determination may become expensive and time-consuming. A simple wind-load model has been incorporated into the present computer program. The user enters a magnitude that defines the wind pressure on a vertical surface normal to the wind direction and a direction that defines the source of the wind, measured in degrees from the X-axis. The normal wind pressure on each membrane element is then computed by scaling the wind magnitude by the cosine of the angle between the wind direction and the outward normal to the current element surface. This model gives zero pressure on horizontal surfaces and suction on leeward surfaces. The application of this model eliminates the necessity of measuring the wind pressure coefficient C_p experimentally and simplifies input data. However, it must be emphasised that this simple procedure is approximate.

Because the membrane cannot resist any compressive stresses, wrinkling will occur and stresses in the elements will be redistributed when the external loads give rise to compressive stresses larger than the initial tensile stresses. The consideration of wrinkling makes the problem materially nonlinear. A procedure to treat element wrinkling is developed to insure that the load analysis is realistic.

The principal stresses σ_1 and $\sigma_2(\sigma_1 > \sigma_2)$ are always calculated and checked in the process of stress analysis. Whether wrinkling occurs or not can be determined as follows:

1. If $\sigma_1 \leq 0$, biaxial wrinkling occurs.
2. If $\sigma_2 \leq 0$ and $\sigma_1 > 0$, uniaxial wrinkling occurs in the second principal direction.
3. If $\sigma_2 > 0$, wrinkling does not occur.

In the case of biaxial wrinkling, the element is inactive and all stresses must be set equal to zero and a diagonal elastic matrix with a very small component is used in the determination of element stiffness matrices. For the uniaxial wrinkling, the task is to ensure that the compressive stress σ_2 does not arise. This is accomplished by setting all components of elastic matrix in the coordinate system of principal stresses to zero except the component corresponding to the first principal stress σ_1 [13].

By way of illustration, Figure 4 shows the deformed configuration of a hexagon tent shown in Figure 2 under a wind load with a speed of 60 mph in the 60° direction, measured from the X-axis. Figures 5 and 6 show the displacement

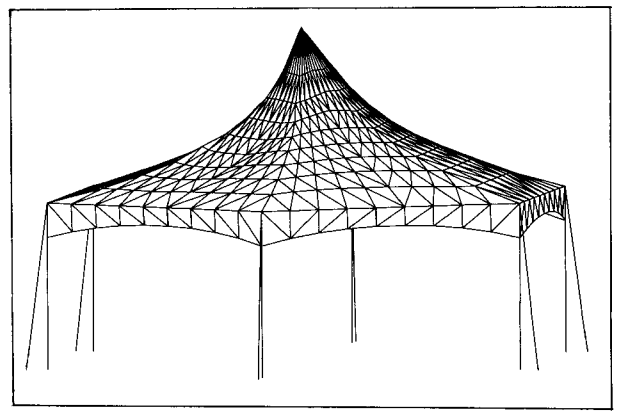

Figure 4. Deformed configuration of hexagon tent.

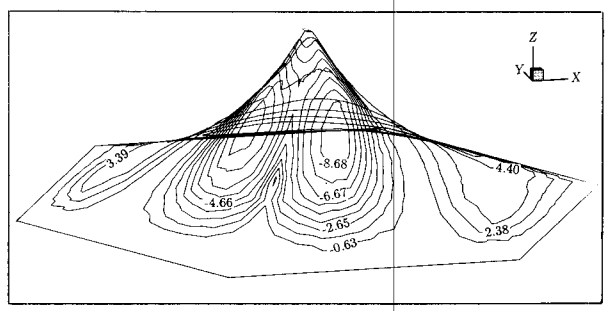

Figure 5. Displacement contours.

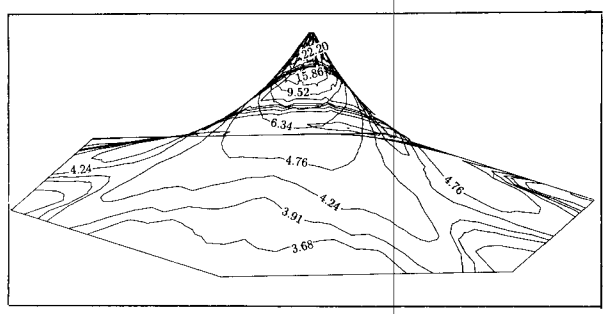

Figure 6. Stress contours.

and stress contours.

For accurate stress distribution in a tension structure under wind loads, dynamic analysis should be performed to take time-dependent wind loads into account [16]. The equations of motion are derived via Hamilton's law of varying action. For the case of small amplitude free vibrations, the system equations determine natural frequencies and vibration mode shapes and take the following eigenvalue form:

$$([\mathbf{K}] - \omega^2[\mathbf{M}])\{\mathbf{u}\} = \{\mathbf{0}\} \ , \qquad (18)$$

where $[\mathbf{M}]$ and $[\mathbf{K}]$ are the system mass and stiffness matrices, and ω is the circular frequency. In free vibration analysis, the stiffness matrix is composed of the elastic matrix, $[\mathbf{K}]_e^l$, and geometric matrix, $[\mathbf{K}]_g^l$, namely:

$$[\mathbf{K}] = [\mathbf{K}]_e^l + [\mathbf{K}]_g^l \ .$$

The eigen-solution approach can be extended for determination of forced oscillations. This requires a transformation from the physical variables $\{\mathbf{u}\}$ to a set of modal variables by means of the system modal matrix. Through this transformation, the equations of motion may be decoupled and solved independently. Finally, the solutions in each mode may be transformed back to the physical variables.

While this approach has its merits, it is limited to linear analysis. The alternative of integrating the equations of motion directly is more general and it allows updating the system matrices at each time step in the numerical integration. If the membrane oscillations are large, the stiffness matrix can change, not only on account of the large changes in geometry, but also because the net stress in an element may become compressive. To account for such nonlinear effects, the nonlinear terms in the strain energy expression must be taken into account. The equations of motion take the following form:

$$[\mathbf{M}]\{\ddot{\mathbf{u}}\} + [\mathbf{K}]\{\mathbf{u}\} = \{\mathbf{R}\} \ . \qquad (19)$$

In Equation 19, $\{\mathbf{R}\}$ is the system nodal force vector. The stiffness matrix takes the form:

$$[\mathbf{K}] = [\mathbf{K}]_e^l + [\mathbf{K}]_g^l + [\mathbf{K}]^{nl} \ ,$$

where $[\mathbf{K}]^{nl}$ is the "nonlinear" stiffness matrix, that is, it is a function of displacements $\{\mathbf{u}\}$. As the geometry of the surface changes, due to large amplitude oscillations, both system matrices will need to be updated from one time step to the next.

CUTTING PATTERN GENERATION

Once a satisfactory shape has been found, a cutting pattern, based on the finite element model for form finding analysis, may be generated. The determination of cutting patterns is basically a geometrical operation to find the shapes of fabric strips, in a plane, which, when joined together, will take the desired shape in 3-D space. With the exception of developable surfaces, all plane cloth geometry determination must be approximate. Tension structures are highly varied in their size, curvature and material stiffness. Cutting pattern approximation is strongly related to each of these factors. It is essential for a cutting pattern generation

method to minimize possible approximations and to produce reliable plane cloth data. The objective is to develop the shapes described by such data, as near as possible to the ideal doubly-curved strips.

In general, cutting pattern generation includes two steps. First, the global surface of a tension structure is divided into individual cloth layout. Second, for each cloth strip, in the three dimensional space an associated plane strip is determined with least distortion, as explained in the following. If a fabric cloth consists of only one layout of elements, the element of the cloth, in the sense of two flat triangles with a fold in between, may be developed to a distortion-free plane form. The corresponding cutting pattern can be found by simply taking each cloth strip and unfolding each triangular element. This exact technique is entirely geometric and is therefore very reliable. The simplest and most commonly used method is termed cloth unfolding. In practice, however, it is necessary to have a constant maximum strip width determined by the fabric width. A mesh with single layout of elements per cloth strip may be not fine enough for the geometrical description of a doubly-curved surface.

A major approximation in the cloth unfolding approach lies in the use of single layout of elements per cloth width. Another problem with cloth unfolding is the typical absence of intermediate nodes at cloth ends. It is necessary to consider that a cloth consists of several layouts of elements in order to accurately simulate the ideal doubly-curved membrane surface and produce usable cutting pattern data. In this case, the subsurfaces cannot be simply unfolded and they must be flattened. For this purpose, a least squares minimization flattening approach is developed to minimize the change in general link length. For each strip, we consider each side of triangular elements as a link element with nodes a and b and minimize:

$$S(\mathbf{x}) = \sum_{i=1}^{m} \phi_i^2(\mathbf{x}) \ , \tag{20}$$

where m is the number of all link elements involved in this strip and $\mathbf{x}$ is the coordinate vector of plane cloth to be determined:

$$\phi_i(\mathbf{x}) = \sqrt{(x_{i,a}-x_{i,b})^2+(y_{i,a}-y_{i,b})^2}-d_i \ , \tag{21}$$

where $(x_{i,a}, y_{i,a})$ and $(x_{i,b}, y_{i,b})$ are the unknown coordinates in the plane for ith link element, and:

$$d_i = \sqrt{(X_{i,a}-X_{i,b})^2+(Y_{i,a}-Y_{i,b})^2+(Z_{i,a}-Z_{i,b})^2} \ , \tag{22}$$

is the actual length of ith link element with 3-D node coordinates $(X_{i,a}, Y_{i,a}, Z_{i,a})$ and $(X_{i,b}, Y_{i,b}, Z_{i,b})$ determined in the form finding procedure.

To ensure that adjacent cloth strips remain compatible after flattening, it is essential that all seam boundary lengths remain unchanged. We give a greater "weight" to those ϕ_i corresponding to the boundary link elements in the following sense: instead of minimizing Equation 20, we minimize:

$$S(\mathbf{x}) = \sum_{i=1}^{m} \omega_i \phi_i^2(\mathbf{x}) \ , \tag{23}$$

where $\omega_i > 0$, $i = 1, 2, \cdots, m$, are factors which determine the "weight" of the different link elements.

The weighted least squares flattening approach is shown to be similar to finite element analysis of truss networks [15]. We can deal with each individual link element by calculating element matrices, the global matrices may then be obtained by assembling all link element matrices. This makes the least squares minimization procedure particularly simple.

The cutting pattern generation starts from the base line specified by the designer. Based on the maximum allowable fabric width, the program searches for geodesic lines and forms a quadrilateral subsurface. Then 3-D mesh is generated for the subsurface and is forced flat. Figures 7 and 8 show geodesic cutting lines of a saddle span tent and typical cutting pattern.

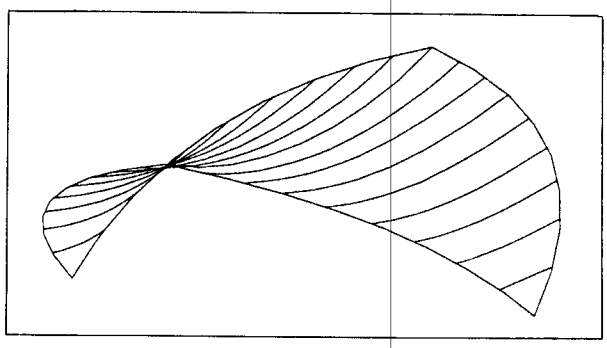

Figure 7. Geodesic cutting lines of saddle span tent.

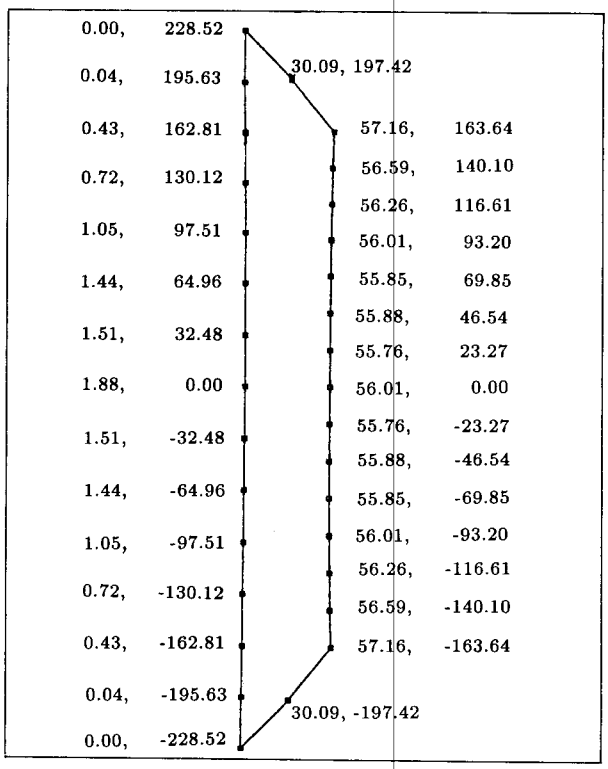

Figure 8. Typical cutting pattern.

CONCLUDING REMARKS

In this paper, a computer method for analysis and design of tension structures has been described. An integrated program package has been developed to perform form finding, load analysis and cutting pattern generation for tension structures. The computed results may be color-graphically presented. The program provides a versatile and powerful tool by means of which the designer may create aesthetically pleasing and structurally sound tension structures.

REFERENCES

1. Argyris, J.H., Angelopoulos, T. and Bichat, B. "A general method for the shape finding of lightweight tension structures", *Comput. Meths. Appl. Mech. Engrg.*, **3**, pp 135-149 (1974).

2. Haber, R.B. "Computer-aided design of cable reinforced membrane structures", Ph.D. thesis, Cornell University (1980).

3. Barnes, M. "Non-linear numerical solution methods for static and dynamic analysis of tension structures", in *Air-Supported Structures*, Institution of Structural Engineers, London (1980).

4. Haber, R.B. and Abel, J.F. "Initial equilibrium solution methods for cable reinforced membranes, part I-formulations, part II-implementation", *Comput. Meths. Appl. Mech. Engrg*, **30**, pp 263-306 (1982).

5. Barnes, M.R. "Computer-aided design of the shade membrane roofs for Expo 88", *Struct. Engng. Review*, **1**, pp 3-13 (1988).

6. Grundig, L. "Minimal surfaces for finding forms of structural membranes", *Proc. Third Inter. Conf. on Civil and Structural Eng.*, Edinburgh (1987).

7. Wakefield, D.S. "Tensyl: an integrated CAD approach to stressed membrane structures", *Proc. Second Inter. Conf. on Civil and Structural Eng.*, Edinburgh (1985).

8. Nishimura, T., Tosaka, N. and Honma, T. "Membrane structure analysis using the finite element technique", in *IASS Symposium*, **2** (1986).

9. Miyamura, A., Tagawa, K., Mizobuchi, Y., Kojima, O., Fujikake, M. and Murata, J. "A case study of the design and construction of tension fabric structures", *Proc. Inter. Colloquium on Space Structures*, Beijing (1987).

10. Contri, P. and Schrefler, B.A. "A geometrically nonlinear finite element analysis of wrinkled membrane surfaces by a no-compression material model", *Communs. Appl. Numer. Meth.*, **4**, pp 5-15 (1988).

11. Fujikake, M., Kojima, O. and Fukushima, S. "Analysis of fabric tension structures", *Computers and Structures*, **32**, pp 537-547 (1989).

12. Moncrieff, E. and Topping, B.H.V. "Computer methods for the generation of membrane cutting patterns", *Computers and Structures*, **37**, pp 441-450 (1990).

13. Tabarrok, B. and Qin, Z. "Nonlinear analysis of tension structures", *Computers and Structures*, **45**, pp 973-984 (1992).

14. Tabarrok, B. and Qin, Z. "A finite element procedure for form finding of tension structures", *Trans. Canada Soc. Mech. Engrg.*, **16**, pp 235-250 (1992).

15. Tabarrok, B. and Qin, Z. "Form finding and cutting pattern generation for fabric tension structures", *Microcomputers in Civil Eng.*, **8**, pp 377-384 (1993).

16. Tabarrok, B. and Qin, Z. "Dynamic analysis of tension structures", submitted to *J. of Sound and Vibration* (1994).

17. Zienkiewicz, O.C. and Phillips, D.V. "An automatic mesh generation scheme for plane and curved surfaces by isoparametric coordinates", *Int. J. Num. Methods Engrg.*, **3**, p 519 (1971).

18. American National Standards Institute, ANSI-A58.1-1982.